

A hybrid Quantum proposal to deal with 3-SAT problem

Jose J. Paulet¹, Luis F. LLana², Hernan I. de la Cruz³, Mauro Mezzini⁴, Fernando Cuartero³, and Fernando L. Pelayo³

¹Qsimov Quantum Computing S.L, Spain

²Complutense university of Madrid, Spain

³University of Castilla - La Mancha, Spain

⁴Roma Tre University, Italy

Going as far as possible at SAT problem solving is the main aim of our work. For this sake we have made use of quantum computing from its two, on practice, main models of computation. They have required some reformulations over the former statement of 3-SAT problem in order to accomplish the requirements of both techniques. This paper presents and describes a hybrid quantum computing strategy for solving 3-SAT problems. The performance of this approximation has been tested over a set of representative scenarios when dealing with 3-SAT from the quantum computing perspective.

1 Introduction

The SAT problem is a well-known NP-complete problem [1] with a wide range of applications in fields such as cryptanalysis [2], hardware verification [3], AI planning [4] and medicine [5]. There are two main approaches to solve the SAT problem from an algorithmic perspective. The first approach is based on the Davis-Putnam-Logemann-Loveland (DPLL) algorithm [6], which uses backtracking as its core mechanism. The second approach is based on *local search* algorithms, which use heuristics to change from one state to another until reaching a valid interpretation.

Examples of local search algorithms include *hill climbing / gradient descent* and *simulated annealing* [7], with the latter being able to leverage the

Jose J. Paulet: paulet@qsimov.com

Luis F. LLana: llana@ucm.es

Hernan I. de la Cruz: HernanIndibil.Cruz@uclm.es

Mauro Mezzini: mauro.mezzini@uniroma3.it

Fernando Cuartero: Fernando.Cuartero@uclm.es

Fernando L. Pelayo: FernandoL.Pelayo@uclm.es

power of annealing quantum computing.

Quantum Annealing, QA, follows a probabilistic algorithm that uses some quantum-mechanical phenomena, such as superposition and tunneling, to search for the global minimum of a given cost function. On practice QA is a powerful optimization technique devoted to deal with some complex problems, most of them combinatorics involving, that are intractable on practice for classical computers.

Adiabatic quantum computing and quantum annealing go hand in hand, but they do not necessarily have to be the same thing. QA does not necessarily require adiabaticity [8]. The time computational complexity of the adiabatic quantum annealing algorithm depends on $T_a \cdot \max_s(|H(s)|)$ [9], where $H(s)$ represents the time-dependent Hamiltonian, and T_a is the total annealing time. This ensures that the minimum energy state can be obtained with high probability as long as the calculation takes place in an ideal closed system, perfectly isolated from the interference of environmental energy.

DWave Quantum annealers supported by quantum fluctuation, return low energy solutions of an objective function. They are mainly used for optimization problems and probabilistic sampling problems. The first problems search for the lowest energy state and the second problems search for good low energy samples.

D-Wave's quantum computers are protected by enclosures that shield them against electromagnetic interference and keeps the operation temperature below 15 mK. However, this is not enough to eliminate interference, which has the general effect of reducing the probability of ending up in a ground state. Additionally, the annealing time T_a is limited to $1 \mu s \leq T_a \leq 2000 \mu s$ which prevent the user from performing in them

arbitrarily slow. Therefore, the theoretical guarantees on performance may not apply to these systems. Thus this technique can just be taken as a heuristic solver, which requires empirical approaches for performance analysis [10].

There exist some undesirable possible effects on the quality of the solution provided by DWave’s quantum annealers as Background Susceptibility, Flux Noise of the Qubits, DAC Quantization, High-Energy Photon Flux, Readout Fidelity and uncontrolled Programming Errors.

Whatever of these optimization problems to be run within a D-Wave’s Quantum Processing Unit, QPU, requires to build a matrix representing a Quadratic Unconstrained Binary Optimization, QUBO, problem. A QUBO problem is a combinatorial optimization problem defined as:

$$\min f(x) = x^T Q x \quad (1)$$

Where x is a column vector of Boolean variables (x_0, \dots, x_{n-1}) and Q is a square matrix of size $n \cdot n$ made of the constants of the problem in question.

A more explicit definition of the problem is:

$$\min f(x) = \sum_{i=0}^{n-1} \sum_{j=1}^i q_{ij} x_i x_j \quad (2)$$

Where $x_i, x_j \in \mathbb{B}$ and $q_{ij} \in \mathbb{R}$ for all $1 \leq j \leq i \leq n - 1$.

Therefore without loss of generality we just consider upper triangular matrices to represent QUBO problems:

$$\begin{pmatrix} q_{00} & q_{01} & \cdots & q_{0n-1} \\ 0 & q_{11} & \cdots & q_{1n-1} \\ \vdots & \vdots & \ddots & \vdots \\ 0 & 0 & \cdots & q_{n-1n-1} \end{pmatrix} \quad (3)$$

These matrices conform the starting point to perform over DWave’s quantum annealers.

Quantum computing based on circuit model is another paradigm that leverages the principles of quantum mechanics to perform computations. It performs over quantum circuits made of interconnected quantum gates that manipulate qubits. This conforms a Turing complete computational paradigm.

The most famous search algorithm within this paradigm is Grover’s algorithm [11]. This algorithm searches for an element in an unordered space taking a time for it which belongs to

$O(\sqrt{N})$, where N is the size of the search space, i.e., the number of elements among which seeking has to be performed. It is conformed of two main steps, the oracle operator, which flips the amplitudes of the states corresponding to the solutions, and the inversion about the mean operator, which amplifies the amplitude of those solution states.

The paper is structured as follows, next section provides an state of the art on quantum computing at dealing with SAT problems, section 3 presents the strategies we propose to deal with 3-SAT. Next two sections give a detailed and reproducible description of the setup we have used in order to empirically validate the proposed strategies and the summary of the results obtained. Section conclusion and future work ends the main contribution of this paper. There are 5 appendices devoted to better illustrate fifth section.

2 Related work

In [12] Quantum annealing features to deal with the Boolean Satisfiability Problem (SAT) are shown. There are some many other proposals based on annealing, both simulated[13] and quantum[14] in order to solve this problem.

Leporati et al. propose in [15] three different algorithms over quantum computing circuit model to address the 3-SAT problem. These algorithms, in essence, leverage quantum parallelism to compute the 3-SAT function for all possible states simultaneously. Cerf et al. deal with SAT problem as an structured search problem in [16]. Focusing on Grover’s inspired approaches we can find a sort of cooperative quantum searching proposed by Cheng et al. in [17]. Zhang et al. in [18] present a hybrid Classical/Quantum perspective to deal with 3-SAT. Yan et al. in [19] present a hybrid quantum approach that build Grover’s oracle by quantum annealing.

Paulet et al. propose in [20] a sort of hybrid Classical/Quantum computing approach supported by a heuristics to lead an incremental strategy to perform partial quantum searches over non-structured domains.

3 Hybrid Quantum approach

We make use of both quantum annealing as local search approach and, a sort of DPLL circuit based quantum computing powered scheme in order to

deal with 3-SAT problem. For the former we have performed computations over DWave’s quantum annealers.

Afterwards, we have reached a quantum state over which Grover’s modified algorithm will finish the search.

More on detail, see fig. 1, QA’s output is considered a first approximation from which we reduce the number of superposed states required by Grover’s algorithm.

Quantum annealers to perform over 3-SAT require that the former statement of the problem is transformed into a Max-3SAT problem (a sort of quantitative version of 3-SAT) as an intermediate domain before conforming a QUBO problem which could be sampled over them.

The corresponding output conforms an initial state for Grover’s modified algorithm from which the solution is faster reachable with respect to existing algorithms that solve 3-SAT.

In particular these latter computations, circuit model-based quantum computing, require:

1. building the quantum oracle that checks the former 3-SAT formula
2. superposing some of the qubits
3. applying Grover’s based algorithm
4. measuring the registry in order to obtain the desired output.

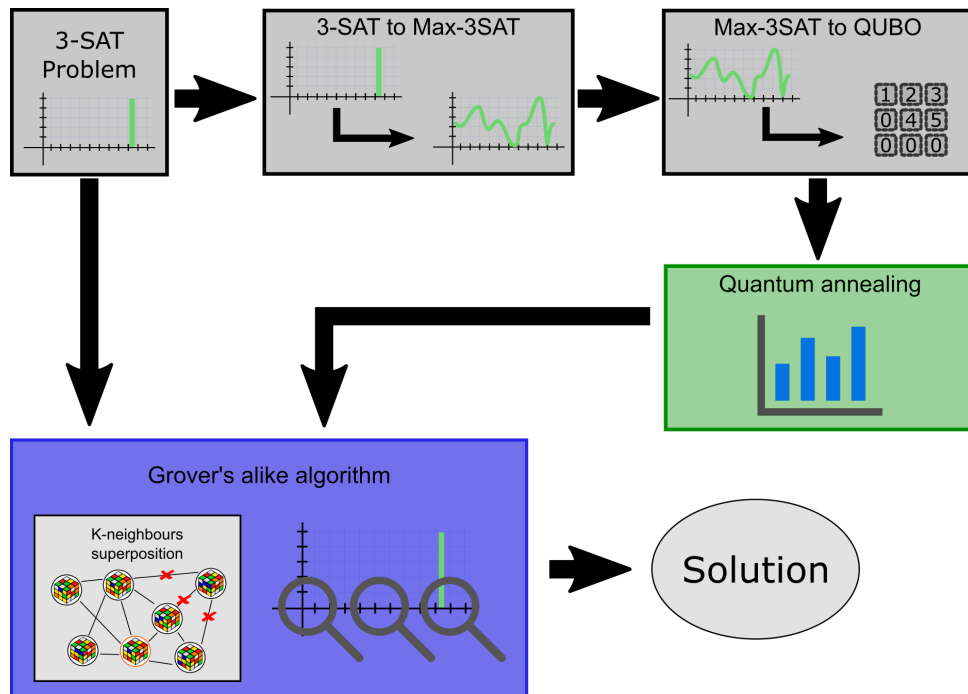


Figure 1: Sketch of the hybrid quantum proposal

3.1 First stage - Quantum annealing

We start using QA as the first approximation to the solution of the problem. In order to do this, a reformulation of the former 3-SAT formula is still required, in particular getting an instance of it as a Quadratic Unconstrained Binary Optimization, QUBO, problem.

Establishing some notation is appropriate in order to describe this process.

Max-SAT¹ is the optimization version of the SAT problem, where the goal is to find the optimal truth assignment based on the maximum number of satisfied clauses, rather than just finding a truth assignment that satisfies a given Boolean formula. We deal with an specific case of weighted Max-SAT (for our case all these weights are set to 1) where weights are assigned to each

¹Unlike the SAT problem, this problem belongs to the class of NP-Hard problems.

clause and the objective remains the same: finding the optimal truth assignment. A more restrictive version of Max-SAT is Max-3SAT that, as 3-SAT refers SAT, specifically refers Max-SAT where each clause has exactly 3 literals.

As in Grover's based algorithms, we focus on problems that have a single solution ($|S| = 1$)

We start evaluating quantitatively how good a truth assignment is for our 3-SAT, instead of evaluating whether the assignment fulfils the Boolean 3-SAT formula. We move to count the number of clauses satisfied by the truth assignment, namely, treat the 3-SAT problem as Max-3SAT problem. It is immediate that valid truth assignments for a given 3-SAT instance produces in the corresponding Max-3SAT the number of clauses that this 3-SAT instance is made of.

Let's see in the following example how this is made on practice: Given the Boolean function f corresponding to a 3-SAT problem:

$$\begin{aligned} f(x_4, x_3, x_2, x_1, x_0) &= (\overline{x_0} \vee \overline{x_1} \vee \overline{x_2}) \wedge \\ &\wedge (x_1 \vee \overline{x_3} \vee \overline{x_4}) \wedge (x_4 \vee \overline{x_2} \vee \overline{x_0}) \wedge \\ &\wedge (x_0 \vee x_1 \vee \overline{x_3}) \wedge (x_1 \vee x_2 \vee x_0) \end{aligned} \quad (4)$$

The corresponding integer function that defines the Max-3SAT problem is:

$$\begin{aligned} f_{max}(x_4, x_3, x_2, x_1, x_0) &= (\overline{x_0} \vee \overline{x_1} \vee \overline{x_2}) + \\ &+ (x_1 \vee \overline{x_3} \vee \overline{x_4}) + (x_4 \vee \overline{x_2} \vee \overline{x_0}) + \\ &+ (x_0 \vee x_1 \vee \overline{x_3}) + (x_1 \vee x_2 \vee x_0) \end{aligned} \quad (5)$$

It is immediate that truth assignment $x_0 = x_2 = x_3 = x_4 = 0$ and $x_1 = 1$ is a model of

the 3-SAT problem:

$$\begin{aligned} f(x_4, x_3, x_2, x_1, x_0) &= (\overline{0} \vee \overline{1} \vee \overline{0}) \wedge \\ &(1 \vee \overline{0} \vee \overline{0}) \wedge (0 \vee \overline{0} \vee \overline{0}) \wedge \\ &\wedge (0 \vee 1 \vee \overline{0}) \wedge (1 \vee 0 \vee 0) = 1 \end{aligned} \quad (6)$$

And the output on the corresponding Max-3SAT equals the number of clauses:

$$\begin{aligned} f_{max}(x_4, x_3, x_2, x_1, x_0) &= (\overline{0} \vee \overline{1} \vee \overline{0}) + \\ &(1 \vee \overline{0} \vee \overline{0}) + (0 \vee \overline{0} \vee \overline{0}) + \\ &+ (0 \vee 1 \vee \overline{0}) + (1 \vee 0 \vee 0) = 5 \end{aligned} \quad (7)$$

On the contrary $x_0 = x_1 = x_2 = x_3 = x_4 = 0$ is neither a model of the 3-SAT:

$$\begin{aligned} f(x_4, x_3, x_2, x_1, x_0) &= (\overline{0} \vee \overline{0} \vee \overline{0}) \wedge \\ &(0 \vee \overline{0} \vee \overline{0}) \wedge (0 \vee \overline{0} \vee \overline{0}) \wedge \\ &(0 \vee 0 \vee \overline{0}) \wedge (0 \vee 0 \vee 0) = 0 \end{aligned} \quad (8)$$

Nor the output in the corresponding Max-3SAT equals the number of clauses:

$$\begin{aligned} f_{max}(x_4, x_3, x_2, x_1, x_0) &= (\overline{0} \vee \overline{0} \vee \overline{0}) + \\ &(0 \vee \overline{0} \vee \overline{0}) + (0 \vee \overline{0} \vee \overline{0}) + \\ &(0 \vee 0 \vee \overline{0}) + (0 \vee 0 \vee 0) = 4 < 5 \end{aligned} \quad (9)$$

From an instance of a Max-3SAT problem we need to move to an optimization function without restrictions for which we follow the process described in [21] and [22]. Each clause is converted into a function (that will be part of the whole optimization function) which strongly depends on the number of negated literals within the clause as following table shows

Negations	Clause	Equivalent function
0	$(x_i \vee x_j \vee x_k)$	$x_i + x_j + x_k - x_i x_j - x_i x_k - x_j x_k + x_i x_j x_k$
1	$(x_i \vee x_j \vee \overline{x_k})$	$1 - x_k + x_i x_k + x_j x_k - x_i x_j x_k$
2	$(x_i \vee \overline{x_j} \vee \overline{x_k})$	$1 - x_j x_k + x_i x_j x_k$
3	$(\overline{x_i} \vee \overline{x_j} \vee \overline{x_k})$	$1 - x_i x_j x_k$

Practically, over our example it produces:

$$\begin{aligned} f'_{max}(x_4, x_3, x_2, x_1, x_0) &= -x_0 x_1 x_3 - x_0 x_1 + \\ &+ x_0 x_2 x_4 - 2x_0 x_2 + x_0 x_3 + x_0 - x_1 x_2 + \\ &+ x_1 x_3 x_4 + x_1 x_3 + x_1 + x_2 - x_3 x_4 - x_3 + 4 \end{aligned} \quad (10)$$

Some cubic terms have been generated at this point. They will be reduced to quadratic by adding some new auxiliary variables together with some penalty functions as stated in [23], i.e., given a cubic term $x_i x_j x_k$ we have to replace the appearances of $x_i x_j$ with the variable y_{ij} and af-

terwards we have to add to the model the penalty function $M(x_i x_j - 2x_i y_{ij} - 2x_j y_{ij} + 3y_{ij})$. This process implies that the number of Boolean variables moves from n in Max-3SAT up to $n + m$ where m refers the number of clauses (which equals the number of cubic terms generated in the previous process *1 per clause at most*). This is an expensive computational process, specially taken into account that we just want to sample the QUBO problem.

Therefore, we have decided to follow the integer programming option proposed by Amit et al. in [24], in advance we take ideas from [21] in order to reduce as much as we can the amount of auxiliary variables.

These latter ideas lead our example to:

$$\begin{aligned} f''_{max}(x_4, x_3, x_2, x_1, x_0) = & -x_0 x_1 + x_0 x_2 x_4 \\ & - 2x_0 x_2 + x_0 x_3 - x_0 y_{13} + x_0 - x_1 x_2 \\ & + x_1 x_3 + x_1 + x_2 - x_3 x_4 - x_3 + x_4 y_{13} + 4 \\ & - M(x_1 x_3 - 2x_1 y_{13} - 2x_3 y_{13} + 3y_{13}) \end{aligned} \quad (11)$$

From it, the integer programming option moves our example to:

$$\begin{aligned} f_{QUBO}(x_4, x_3, x_2, x_1, x_0) = & -x_0 x_1 - 2x_0 x_2 \\ & + x_0 x_3 - x_0 y_{13} + x_0 - x_1 x_2 + x_1 x_3 + x_1 \\ & + x_2 - x_3 x_4 - x_3 + x_4 y_{02} + x_4 y_{13} + 4 \\ & - M(x_1 x_3 - 2x_1 y_{13} - 2x_3 y_{13} + 3y_{13}) \\ & - M(x_0 x_2 - 2x_0 y_{02} - 2x_2 y_{02} + 3y_{02}) \end{aligned} \quad (12)$$

To finish with, proper value for M is computed, according to [21], as $M = 1$. The definite version of f_{QUBO} which coefficients can be directly mapped into DWave QPUs is

$$\begin{aligned} f_{QUBO}(x_4, x_3, x_2, x_1, x_0) = & -x_0 x_1 - 3x_0 x_2 \\ & + x_0 x_3 + 2x_0 y_{02} - x_0 y_{13} - x_1 x_2 + 2x_1 y_{13} \\ & + x_0 + x_1 + 2x_2 y_{02} + x_2 - x_3 x_4 + 2x_3 y_{13} \\ & - x_3 + x_4 y_{02} + x_4 y_{13} - 3y_{02} - 3y_{13} + 4 \end{aligned} \quad (13)$$

3.2 Second/Last stage - Quantum circuit model

Once QA has provided its output it is time to describe the quantum circuit-model search algorithms. By this second computation we search

for neighbour states based on both Hamming distance and on a sort of cyclical distance. From now on, we will call them *Quantum Hamming search* and *Quantum Cyclical search*.

Henceforth, S denotes the set of solution states of the problem in question and, \bar{S} stands for the non-solution states set of that problem.

3.2.1 Quantum Hamming search

It is a quantum computing searching process over Hamming distance, see [25]. It starts on a given quantum state and searches in its Hamming surroundings. Its inputs are:

- Number of qubits of the state: n
- Initial state from which starts computations: $|\gamma\rangle$ (which has been provided by previous QA computing)
- Integer value k taken, within Grover's algorithm, as tentative Hamming distance to solution.

Since the correct value for k is not known until finishing the whole search we will denote by k_f the Hamming distance between $|\gamma\rangle$ and the state $|\tau\rangle$ that names the solution of the 3-SAT problem under consideration.

This third parameter k will be increased iteratively from $k = 1$ until measuring the solution as output of the corresponding Grover's instance. Notice that these values for k hold $k \leq k_f$.

Let's see on detail how does it work:

As usual, an initial superposition is made. In our case the following H_α operator is applied to each input qubit:

$$H_\alpha = \begin{pmatrix} \sqrt{1 - \frac{1}{\alpha}} & \sqrt{\frac{1}{\alpha}} \\ \sqrt{\frac{1}{\alpha}} & -\sqrt{1 - \frac{1}{\alpha}} \end{pmatrix} \quad (14)$$

Where α is $\frac{n}{k}$ and k is the Hamming distance that we are checking.

This operator performs a non-uniform superposition, that benefits the k -nearest states. The resulting probability amplitude of a state at a distance k (either it corresponds to a solution or not) is:

$$amp_\alpha = \sqrt{\left(1 - \frac{k}{n}\right)^{n-k_f}} \cdot \sqrt{\left(\frac{k}{n}\right)^{k_f}} \quad (15)$$

Afterwards, the amplitude amplification operator is required:

$$IAM_\alpha = 2 \cdot H_\alpha^{\otimes n} |\gamma\rangle \langle \gamma| H_\alpha^{\dagger \otimes n} - I_n \quad (16)$$

In a nutshell, the corresponding quantum circuit (once a non-measurable -1 global phase has been added) is that depicted in fig. 2:

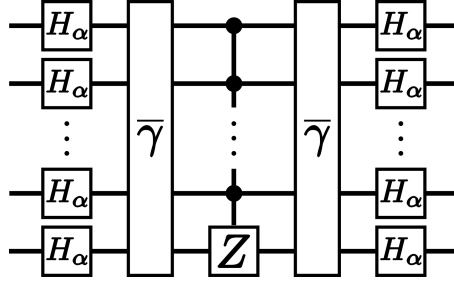


Figure 2: Inversion about the mean (Hamming distance)

Our algorithm executes t_α times the Grover's iterative operator G_α defined as follows:

$$G_\alpha = (2 \cdot H_\alpha^{\otimes n} |\gamma\rangle \langle \gamma| H_\alpha^{\dagger \otimes n} - I_n) \cdot U_f \quad (17)$$

Where U_f refers, as usual, the quantum oracle that just inverts the sign of the solution state.

Regarding the initial superposition, let us notice that the angle between the no solution states $|\bar{S}\rangle$ and the initial superposition $|\psi_\alpha\rangle$ is θ_α as it is shown in fig 3.

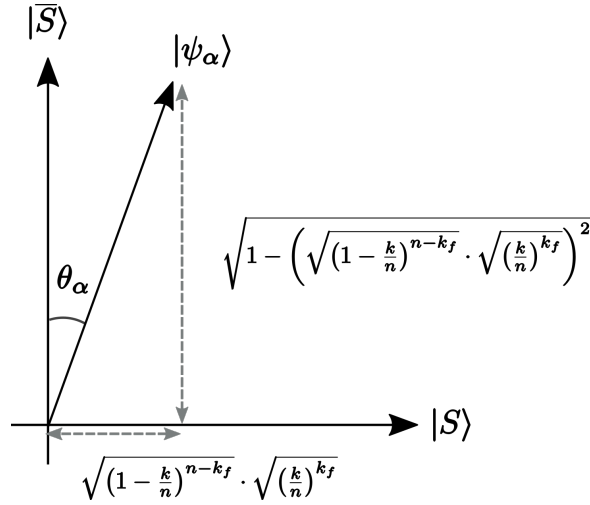


Figure 3: Graphical representation of the initial superposition (Quantum Hamming search)

Therefore:

$$\theta_\alpha = \sin^{-1} \left(\sqrt{\left(1 - \frac{k}{n}\right)^{n-k_f}} \cdot \sqrt{\left(\frac{k}{n}\right)^{k_f}} \right) \quad (18)$$

It is straightforward that each iteration involves a rotation of $2 \cdot \theta_\alpha$, from which the probability amplitude of a solution state after t_α iterations will be:

$$amp_{t_\alpha} = \sin(\theta_\alpha \cdot (2 \cdot t_\alpha + 1)) = \sin \left(\sin^{-1} \left(\sqrt{\left(1 - \frac{k}{n}\right)^{n-k_f}} \cdot \sqrt{\left(\frac{k}{n}\right)^{k_f}} \right) \cdot (2 \cdot t_\alpha + 1) \right) \quad (19)$$

In order to calculate the number of iterations

required to measure the solution state with a

probability acceptably close to 1, we force the following condition to be met:

$$\theta_\alpha (2 \cdot t_\alpha + 1) = \frac{\pi}{2} \quad (20)$$

From which we can compute t_α :

$$t_\alpha = \frac{\pi}{4 \cdot \sin^{-1} \left(\sqrt{\left(1 - \frac{k}{n}\right)^{n-k_f}} \cdot \sqrt{\left(\frac{k}{n}\right)^{k_f}} \right)} - \frac{1}{2} \quad (21)$$

As previously stated, value of k_f is not known in advance for which we assume within each iteration that the Hamming distance we are considering is the right one, which implies $k_f = k$ and consequently with this assumption we compute the number of iterations to be performed at this time as $\text{Round}(t_\alpha)$, i.e., $\lfloor t_\alpha \rfloor$.

These $\lfloor t_\alpha \rfloor$ are the values to be added per each value of k , in order to get the key element to be compared.

3.2.2 Quantum Cyclical search

The original Grover's algorithm uses the Walsh-Hadamard transformation to search all along the problem domain.

Some other quantum searching algorithms, see [25, 26], do replace the Walsh-Hadamard transformation within this task.

In particular, we support our proposal on a replacement of this transformation by a kind of neighbourhood search. In particular this neighbourhood is defined over a cyclical distance which will be defined in subsection 4.4.

This algorithm searches among the 2^r closest states to the state $|\gamma\rangle$ provided in first stage, i.e., it first searches in the states $[(\gamma - 2^{r-1} + 1) \bmod 2^n, (\gamma + 2^{r-1}) \bmod 2^n]$ for the first iteration (corresponding to the states which distance belongs to $[0, 2^{r-1}]$), then it searches in the next 2^r closest states to $|\gamma\rangle$ avoiding previously searched states (corresponding to the states having a distance belonging to $(2^{r-1}, 2^r]$), and so on.

As a matter of example, the distance between state 0 and state $2^n - 1$ is just 1 as a consequence of our cyclical assumption *mod* 2^n .

Let us describe, in an algorithmic way, how the corresponding superposition on the quantum states could be generated.

We have named *Range splitter operator* (U_r), which quantum circuit representation is shown in fig. 4, the piece of quantum code responsible for this task.

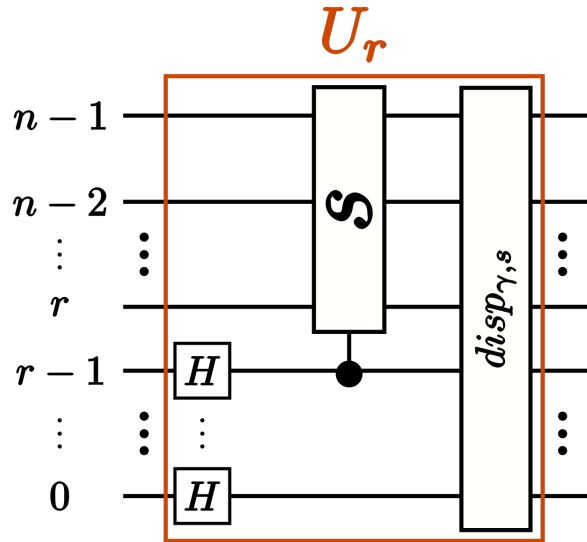


Figure 4: Range splitter operator

This operator superposes a total of 2^r states in two eventually non-consecutive ranges. In fact, they will be located at a distance of $s \cdot 2^r$ states, where $s \in \mathbf{N}$.

This operator first superposes some qubits in order to generate the two ranges which relative location is the following one:

$$[0, 2^{r-1} - 1] \cup [(s + \frac{1}{2}) \cdot 2^r, (s + \frac{1}{2}) \cdot 2^r + 2^{r-1} - 1] \quad (22)$$

Fig. 5 shows these pairs of ranges (after the corresponding displacement which will be described

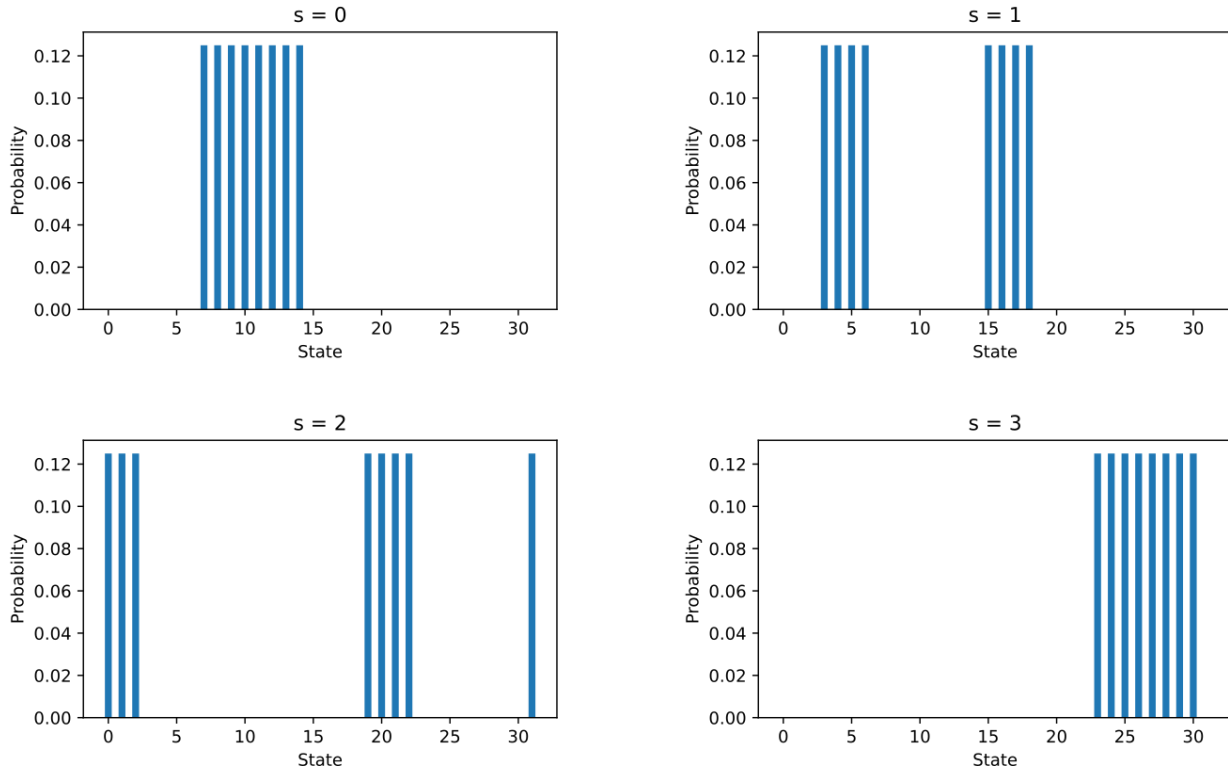


Figure 5: Example of superposition with $\gamma = 10$, $r = 3$, $n = 5$ and $s = 0, 1, 2, 3$

In contrast with the most of the iterative quantum searching methods, our proposal fully avoids repetitions, i.e., it ranges over disjoint domains. Let's see on detail how does this superposition generates more and more distant ranges of neighbours, is achieved:

Hadamard gates in fig. 4 create a superposition of the first (from least to most significant) 2^r states:

$$\sum_{x_0, \dots, x_{r-1} \in \{0,1\}} \frac{1}{\sqrt{2^r}} \cdot \underbrace{|00 \dots 0 x_{r-1} \dots x_0\rangle}_n \quad (23)$$

First the biggest 2^{r-1} states, i.e., ($|00 \dots 01 x_{r-2} \dots x_0\rangle$) are shifted by an amount of $s \cdot 2^r$. Performing this addition makes use of quantum parallelism in the following way. The states to which we need to perform the addition (most significant states) have in common that

below) in their absolute (proper) location around $|\gamma\rangle$. Please notice that although $|\gamma\rangle$ corresponds to 10^{th} state, for the sake of keeping pure disjoint ranges the exact median over which we have defined and built our ranges is an state between 10^{th} and 11^{th} ones.

their qubit in r^{th} position, (x_{r-1}), is set to $|1\rangle$. This qubit will act as control qubit for adding the value $s \cdot 2^r$ only to the most significant qubits.

These additions make use of a set of *full adders*² to perform the operation.

Taking into account that:

- Full adders are performed by means of **XOR** (\oplus) operator (which neutral element is 0).
- We are adding $s \cdot 2^r$ (which is a multiple of 2^r and therefore its $r - 1$ least significant qubits are set to 0)
- Full adders are applied to the $n - r$ most significant qubits which are set to 0

²Logical circuits that add two bits and an input carry in order to produce a sum and an output carry

$$(|00\dots 01x_{r-2}\dots x_0\rangle)$$

Value $s \cdot 2^r$ can be added to the values 0 just setting the values 1 with controlled X gates on the $n - r$ most significant qubits. These values 1 correspond to those values 1 appearing in the binary representation of $s \cdot 2^r$. Previous computations are equivalent to simply set the value of s (binary encoded) on the $n - r$ most significant qubits (second column in fig 4).

Only displacements remain in order to finish U_r performing description. To do this, at iteration s , we need to perform a displacement (which depends on the QA output state $|\gamma\rangle$) of $disp_{\gamma,s} = \gamma - (s + 1) \cdot 2^{r-1} + 1$. This is achieved by means of performing $(+1)$ quantum gates that operates $+1 \bmod 2^n$ on an n -qubit register. These increments are carried out as described in [27].

On practice, $disp_{\gamma,s}$ is decomposed into as

many increments as values 1 appear within the binary representation of the displacement. Each of these qubits (x_i) will apply the increment quantum gate shown in fig.6 in the way which is described in fig.7. As an example figs. 8 and 9 show on detail the case where the initial state is 13 $|01101\rangle$ and a displacement of 5 is required ($x_4x_3x_2x_1x_0 = 00101$). The number of increments required for this equals the number of variables set to 1, which is 2 (coming from $x_2 = x_0 = 1$). Regarding how these increments must be performed let's say that applying the increment corresponding to $x_2 = 1$ results in an increment for the three most significant qubits, whereas the increment corresponding to $x_0 = 1$ results in an increment for the five most significant qubits, i.e., for all the qubits under consideration.

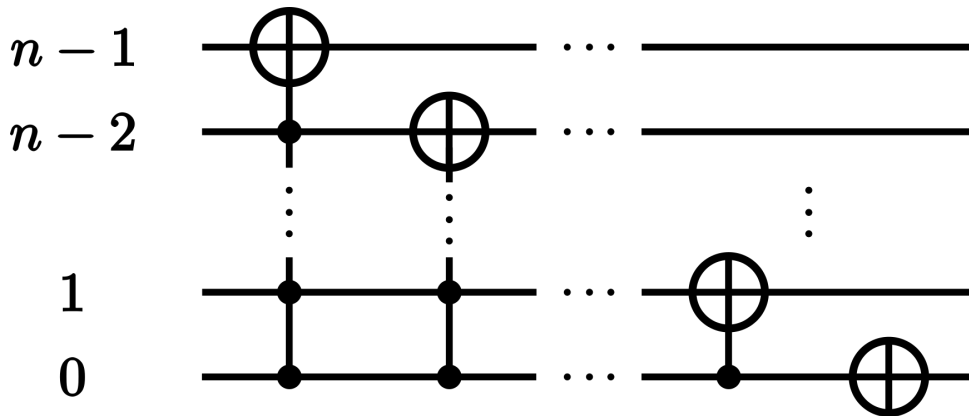


Figure 6: Incremental gate circuit

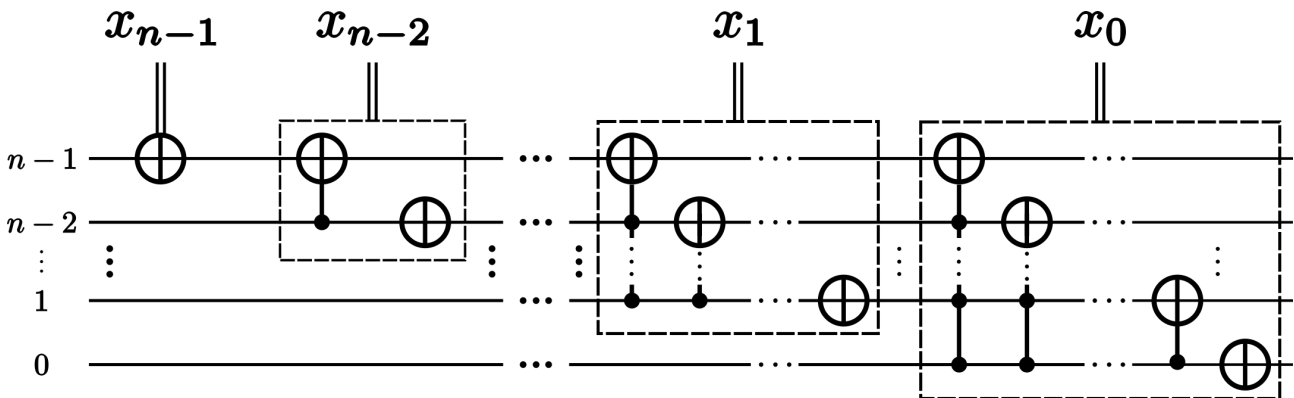


Figure 7: Displacement gate circuit made of Incremental gates ones

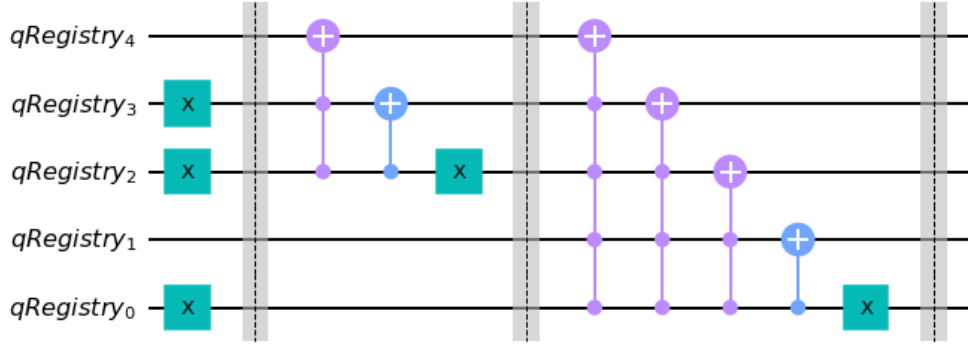


Figure 8: Example of a *Displacement quantum gate circuit* over Qiskit.

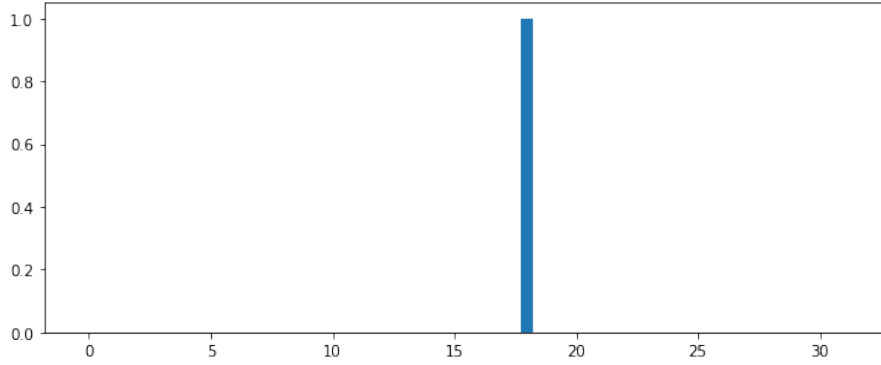


Figure 9: The final probability distribution of the example over Qiskit.

U_r operator so defined is used by the inversion about the mean (IAM_r) operator as follows:

$$IAM_r = 2 \cdot U_r |0\rangle \langle 0| U_r^\dagger - I_n \quad (24)$$

Fig. 10 depicts, on detail, its corresponding quantum circuit, once again the suitable -1 global phase has been added.

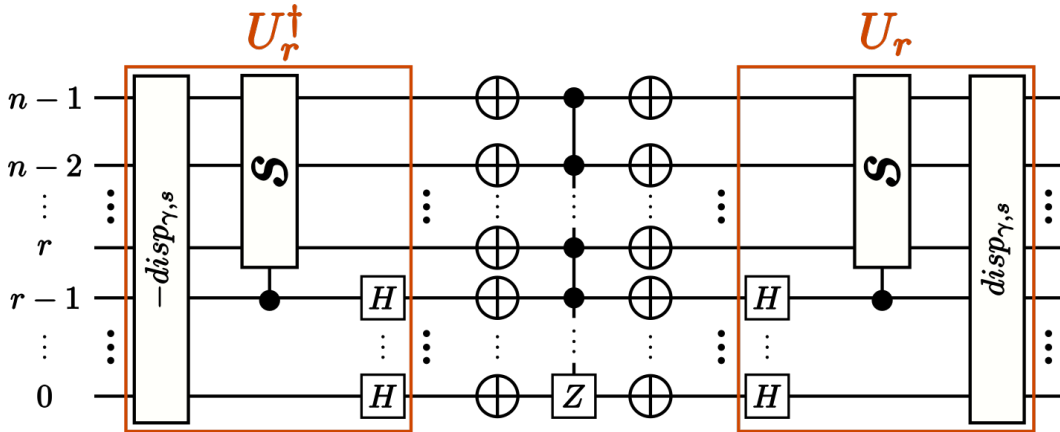


Figure 10: Inversion about the mean (Cyclical distance)

The algorithm we propose consists on iterating t_r

times the operator G_r , that is defined as:

$$G_r = \left(2 \cdot U_r |0\rangle \langle 0| U_r^\dagger - I_n \right) \cdot U_f \quad (25)$$

The number of iterations t_r needed to reach a probability of measuring the solution state close to 1 can be computed as:

$$t_r = \frac{\pi}{4 \left(\sin^{-1} \left(\sqrt{\frac{|S|}{N}} \right) \right)} - \frac{1}{2} \quad (26)$$

Where N is the total number of states in superposition, $|S| = 1$ as previously stated is the total number of solutions. Notice that the total number of states value comes from $N = 2^r$. Therefore we get:

$$t_r = \frac{\pi}{4 \left(\sin^{-1} \left(\sqrt{\frac{1}{2^r}} \right) \right)} - \frac{1}{2} \quad (27)$$

from which the number of iterations required is $\text{Round}(t_r)$, i.e. $\lfloor t_r \rfloor$.

Again, $\lfloor t_r \rfloor$ are the values to be added in order to get the key element to be compared.

4 Testing scenario

For the sake of giving the most details for reproducibility this section is divided into:

- Test cases
- QUBO models & Quantum Annealing
- Quantum Hamming and Cyclical searches

4.1 Test cases

Some preliminary definitions are required:

- The density of a given k-SAT formula $S_f = \bigwedge_{i=1}^m C_i$ is denoted as $d(S_f)$ and defined as the ratio between its number of clauses (m) and its number of Boolean variables (n):

$$d(S_f) = \frac{m}{n}$$

On the related literature it is assumed that $\forall k > 1, k \in \mathbb{N}$ there exists a threshold value for the density of k-SAT formulas d_k such that:

- The farther $d(S_f)$ is from d_k , the fewer calls to the DPLL algorithm [6]) are required to solve the k-SAT problem.
- If $d(S_f) > d_k$ the formula would be unsatisfiable with high probability but just the opposite occurs when $d(S_f) < d_k$, i.e., high

$d(S_f)$ is usually associated with an unsatisfiable formula.

- Mitchell, Selman and Levesque estimated in 1991, see [28], that $d_3 \sim 4.55$ for about 20 variables and $d_3 \sim 4.3$ for larger number of variables.

Regarding our scenario for the tests:

1. The process of generating test cases has been supported by **CNFgen**[29]. A test case for us is a pair (density, number of variables). In particular, 10 3-SAT problems have been generated for each test case.

Supported by those results by Mitchell et al., [28], we have considered 4, 4.3 and 4.55 as most challenging density values.

The number of variables ranges from 7 to 22 (for less than 7 variables annealing algorithms reach the 3-SAT solution easily by themselves whereas the upper threshold of 22 variables has been chosen because together with the high computational cost, we have found neither evidence nor hints that make us suspecting that the advantage we would get beyond 22 could be smaller). Therefore, it computes $3 \cdot 16$ different test cases which computes in total 480 3-SAT problems.

2. In addition to these 480 3-SAT problems, 5 random seeds has been also involved within the setup for the sake of maximum representativity, thus $5 \cdot 10 \cdot 3 \cdot 16 = 2400$ different executions over simulated annealing algorithm have been performed.

The number of iterations required by the algorithm to reach a probability of measuring a solution state close to 1, has been chosen as the parameter of study in order to compare the computational efficiency of the proposed algorithm.

The scenarios we had in mind at the beginning were the first 3 in tab. 1 but due to the low quality of the quantum annealing solutions we have added the last 2 which cover simulated annealing instead of quantum annealing.

Scenario	Annealing algorithm	Circuit quantum search algorithm
1	Not applicable	Grover's algorithm
2	Quantum annealing	Quantum Hamming search
3	Quantum annealing	Quantum Cyclical search
4	Simulated annealing	Quantum Hamming search
5	Simulated annealing	Quantum Cyclical search

Table 1: Scenarios meaning

4.2 QUBO models & Quantum Annealing

The QUBO models and the results we have generated and analysed are available in this repository [30].

This annealing algorithms part just seek to save temporal complexity on the pure quantum computing searching process. To do this, we have calculated the average time it took to execute both annealing algorithms (quantum and classical) on the 10 examples of each test case.

For both quantum annealing and simulated annealing, the temporal complexity is linear as we can see in detail in the Appendices A and B, respectively.

For performing these experiments, we have made use of the software development kit (SDK) provided by DWave (Ocean). Specifically, for the simulated annealing algorithm, we have used the *dwave-neal* library and its sampler *SimulatedAnnealingSampler*. For the quantum annealing execution, we have used the cloud service *Leap* from DWave along with its SDK, and the *dwave-system* library, which contains the *DWaveSampler* for running on the Quantum Processing

Units (QPUs).

To calculate the number of iterations that we would perform in each of the 2 versions of quantum search without simulating the circuits (since we cannot simulate them for more than 6 variables), we will calculate the Hamming distance (k_f) and cyclical distance (d_f) between the solution provided by the annealing algorithms and the real solution to the problem in question. Thus, once this distance is known we will be on condition to calculate the number of iterations that we will perform in each case to obtain the real solution starting from the solution provided by the annealing stage.

4.3 Applying Quantum Hamming search

As previously stated the number of Grover iterations to be performed t_α depends on $\frac{n}{k}$ and on k_f . For estimating k_f we will iteratively execute the algorithm for the values of k in $\{1, \dots, k_i, \dots, k_f\}$ until we get a probability of measuring the solution state greater or equal than 90%.

The probability of measuring the solution state within the first k_i attempts ($k_i \leq k_f$) where the distance to actual solution is k_f , is referred as $P_{sol}(k_i, k_f, n)$ and computed in this way:

$$P_{sol}(k_i, k_f, n) = 1 - \prod_{k=1}^{k_i} \left(\underbrace{1 - \left(\sin \left((2 \cdot \lfloor t_\alpha \rfloor + 1) \cdot \sin^{-1} \left(\sqrt{\left(1 - \frac{k}{n}\right)^{n-k_f}} \cdot \sqrt{\left(\frac{k}{n}\right)^{k_f}} \right) \right)}_{\text{non solution probability}} \right)^2 \right) \quad (28)$$

solution probability

Where t_α comes from equation 21 and $\lfloor \chi \rfloor$ stands for *Round*(χ) (round approximation).

Due to the fact that the probability of measuring one state or another does not depend on previous runs of the algorithm, the probability

after k_i executions equals 1 minus the product of measuring a non-solution in each of the previous independent events (each algorithm's run). Therefore, the total number of iterations needed in a real case according to this Hamming search will be:

$$t_{H_{total}} = \sum_{k=1}^{k_i \leq k_f} \left[\frac{\pi}{4 \cdot \sin^{-1} \left(\sqrt{\left(1 - \frac{k}{n}\right)^{n-k_f}} \cdot \sqrt{\left(\frac{k}{n}\right)^{k_f}} \right)} - \frac{1}{2} \right] \quad (29)$$

Where $k_i = \mu z.P_{sol}(z, k_f, n) \geq 0.9$ where $z \in \mathbb{Z}$.

4.4 Applying Quantum Cyclical search

For the quantum search algorithm based on a sort of cyclical distance, we first need to determine the number of qubits to be superposed, r out of the total number of qubits in the system n (where $N = 2^n$ is the total number of states under consideration). We would like to set r to the minimum value which generates a range that can reach the solution state from the state provided by QA, $|\gamma\rangle$.

The cyclical distance we are considering is defined as follows:

$$d_c(|\gamma\rangle, |\tau\rangle) = \min \{ |\gamma_2 - \tau_2|, 2^n - |\gamma_2 - \tau_2| \} \quad (30)$$

For example,

$$\begin{aligned} d_c(|0010\rangle, |1101\rangle) &= \\ &= \min \{ |(0010)_2 - (1101)_2|, \\ &\quad 2^4 - |(0010)_2 - (1101)_2| \} = \\ &= \min \{ |2 - 13|, 16 - |2 - 13| \} = 5 \end{aligned} \quad (31)$$

which is graphically depicted in fig.11.

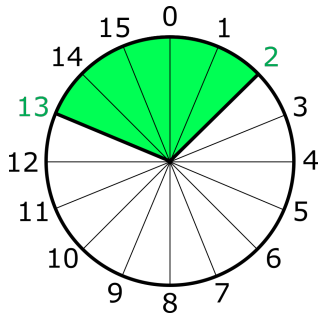


Figure 11: Cyclical distance between $|0010\rangle$ and $|1101\rangle$

As, obviously, the location of the solution state is not known until the algorithm has finished but we need to estimate the total number of iterations indeed, we are forced to find the solution of the SAT problem by brute force, afterwards computing the cyclical distance between it and the output of QA, d_f , in order to keep on with this comparative study.

As stated we are required to know the total number of iterations $t_{C_{total}}$ in each test case, for which we start setting $r = n - 1$ (which covers half of the whole domain per execution). Starting with $r = n - k$ (covering a $1/2^k$ of the whole domain per execution) conforms other possible options. Our decision is just supported by empirical issues.

Therefore, d_f must be divided by the number of states covered in any of the ranges previously defined. Thus, from state $|\gamma\rangle$ we cover $s \cdot 2^{r-1} - 1$ states to the left and $s \cdot 2^{r-1}$ states to the right (because of symmetry issues already pointed out in previous section 3.2.2). Therefore, the number of algorithm executions s_f to be performed (corresponding to former parameter s) is:

$$s_f = \begin{cases} \left\lceil \frac{d(\gamma, \tau) + 1}{2^{r-1}} \right\rceil & \text{if } \gamma \geq \tau \\ \left\lfloor \frac{d(\gamma, \tau)}{2^{r-1}} \right\rfloor & \text{if } \gamma < \tau \end{cases} \quad (32)$$

Consequently, the total number of iterations will be:

$$t_{C_{total}} = \sum_{i=0}^{s_f} \left[\frac{\pi}{4 \left(\sin^{-1} \left(\sqrt{\frac{1}{2^r}} \right) \right)} - \frac{1}{2} \right] \quad (33)$$

This parameter $t_{C_{total}}$ together with $t_{H_{total}}$ are the final parameters that we understand best describe the computational cost of both Quantum Search proposals, and therefore the right ones to be compared.

5 Summary of Results

To begin with, we want to mention that as it is well known that the hard achievability to actual quantum computers in addition to the strong dependency on the topology of the computer, on the circuit optimization, as well as on the characteristics of the quantum gates makes almost impossible to empirically measure times of execution. Instead, the number of iterations within the Grover's alike algorithm are considered as proper size of the problem for comparisons.

Besides, DWave’s quantum annealers execution time depends on two main parameters: the *anneal_schedule* (or *annealing_time*), and the number of executions (*num_reads*). Similarly to quantum circuit model the variability associated to the offer of hardware makes almost impossible to establish criteria in order to accurately compare efficiency of these two different quantum computing models.

In front of the previous scenario we have focused on the fact that quantum searches grows exponentially meanwhile quantum annealing grows linearly, therefore we consider as main

parameter to be considered for comparisons just the usual one for this task within circuit model quantum search, i.e. the number of Grover’s iterations.

Some preliminary considerations regarding quantum annealing and simulated annealing must be stated. We started evaluating the quality/accuracy of these annealing processes according to both Hamming and Cyclical metrics. In order to do this, we compare the distances from the solution state offered by QA $|\gamma\rangle$ and the actual solution state of the former 3-SAT problem $|\tau\rangle$.

Hamming distance comparison between simulated and quantum annealing

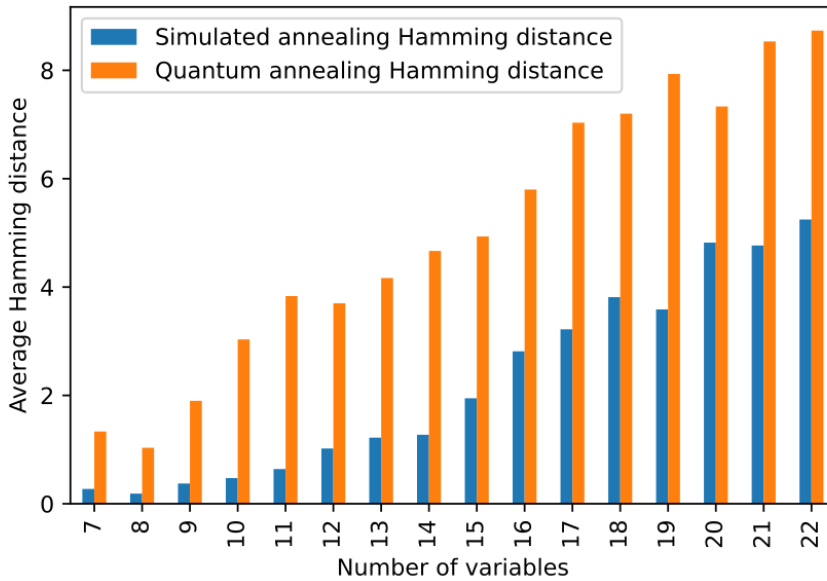


Figure 12: Simulated annealing vs. Quantum annealing Hamming accuracy

As fig.12 shows Simulated Annealing is far more accurate than Quantum Annealing according to Hamming distance. This is quite remarkable as it

strongly affects the subsequent Quantum Search.

Fig.13 compares that accuracy with respect to Cyclical distance. Let us notice that vertical axe follows a logarithmic scale.

Cyclic distance comparison between simulated and quantum annealing

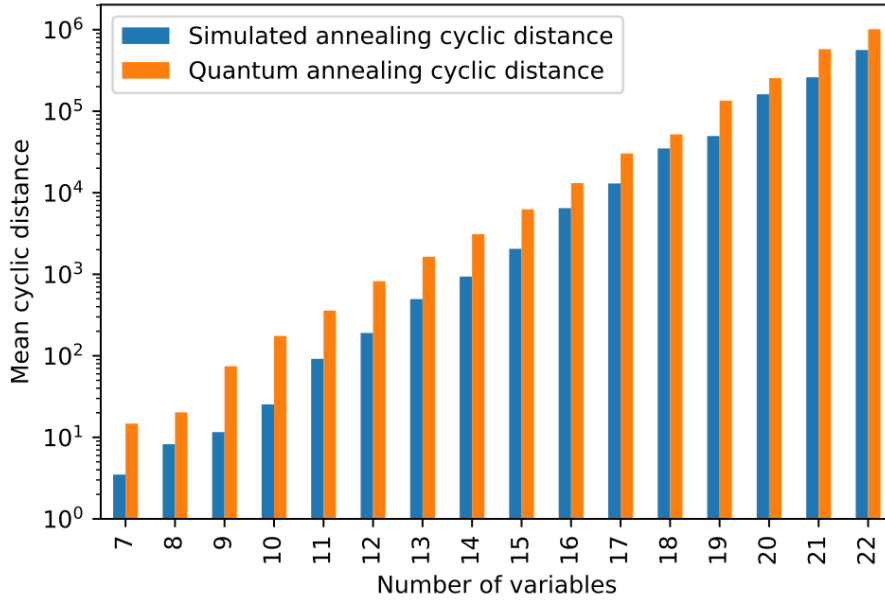


Figure 13: Simulated annealing vs. Quantum annealing Cyclical accuracy

In the same way, Simulated Annealing clearly overcomes Quantum Annealing accuracy according to Cyclical distance.

More detailed figures of the experiments performed for this sake can be found in the table

within appendix C.

Previous results led us to focus on scenarios 1, 4, and 5 of tab.1 until any further Quantum Annealer improves the accuracy of the Simulated Annealing at disposal.

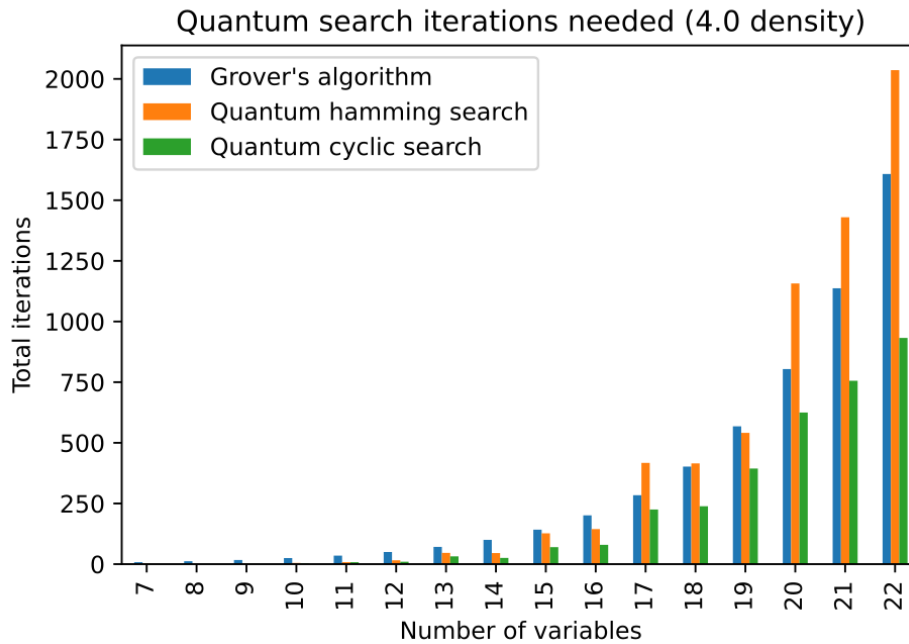


Figure 14: Total number of iterations required in scenarios 1, 4 and 5 over a 3-SAT formula with density 4.0

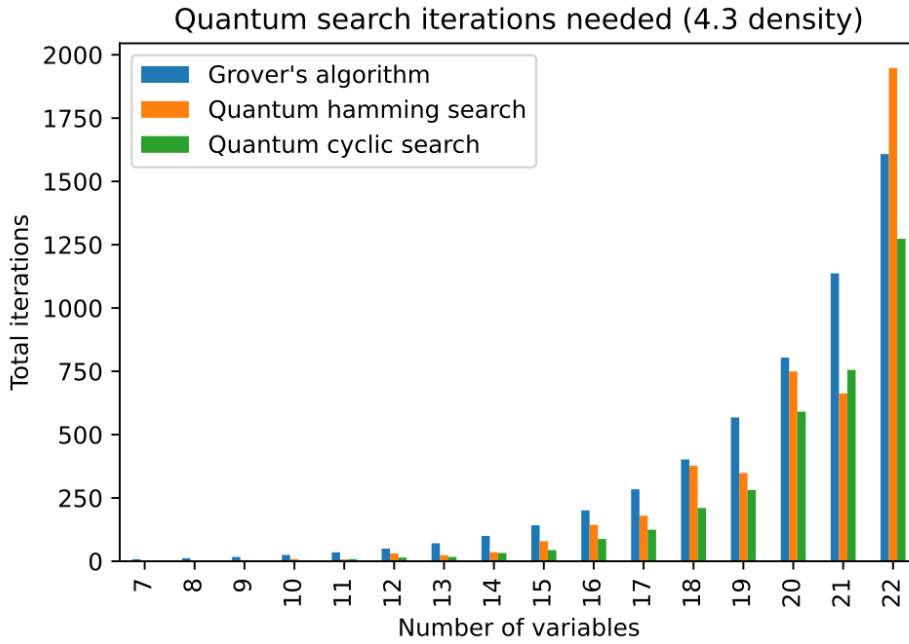


Figure 15: Total number of iterations required in scenarios 1, 4 and 5 over a 3-SAT formula with density 4.3

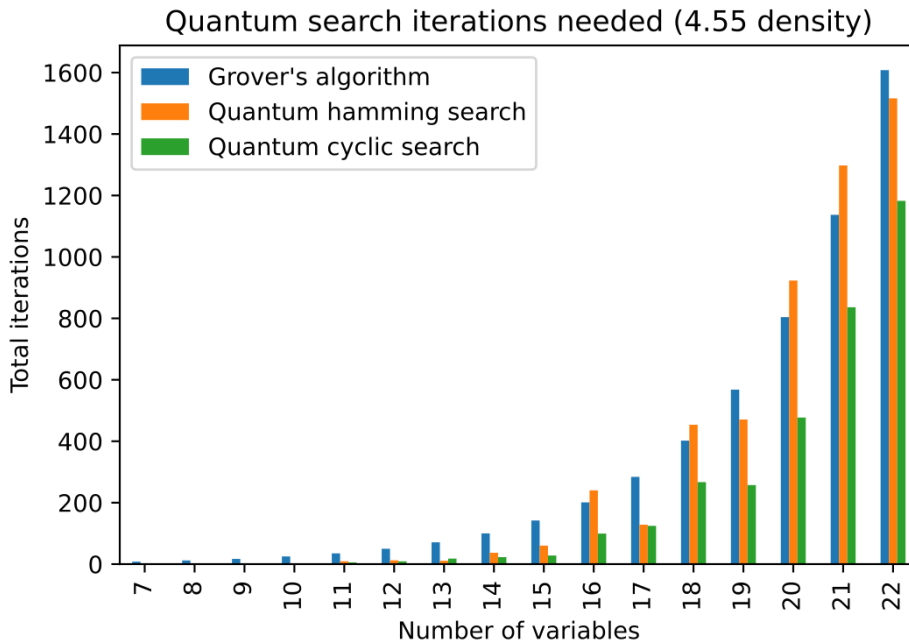


Figure 16: Total number of iterations required in scenarios 1, 4 and 5 over a 3-SAT formula with density 4.55

Graphs depicted on figs. 14, 15 and 16 summarize, stratified by density of the SAT formulas under consideration, the results obtained in our test cases for comparing the two proposed metrics. We can conclude from them on one hand that Hamming search proposal does not improve in general the former Grover quantum

Search, on the other hand Cyclical search proposal clearly improves Grover's algorithm performance though.

We think that the main reason for this relies on the disjoint domains search which is just achievable by cyclical search.

Appendix D includes tabs. 3 and 4 which con-

tain the raw numbers obtained in the comparative tests that we have performed.

Such improvement reaches in the very worst case, i.e. density around 4.3, a saving of one fifth of the number of iterations with respect to the former Grover algorithm.

6 Conclusions and future work

The main contributions of the paper are:

- We have provided a hybrid quantum computing proposal to deal with 3-SAT problem.
- We have provided and compared a couple of metrics which generate a couple of circuit model quantum searching processes the Grover's one alike, i.e. Quantum Hamming and Cyclical Searches.
- We have concluded that it clearly deserves to first approximate 3-SAT problem solving by quantum annealing sampling and then apply quantum cyclical search than just applying Grover's algorithm from scratch.

For future work we think that it could be interesting:

- Studying and developing heuristic approaches for selecting the appropriate values of the distance parameters (k and r) in Quantum Hamming search and Quantum Cyclical search algorithms, respectively.
- Investigating the Reverse Annealing Technique as it empowers users to define the problem they intend to solve and to provide an anticipated solution, thereby narrowing down the search space during the computation process.
- Exploring Anneal Offsets because in some problem scenarios, it can result in an advantage for specific qubits to undergo annealing slightly before or after others.

References

- [1] Stephen A Cook. "The Complexity of Theorem-Proving Procedures". In Proceedings of the Third Annual ACM Symposium on Theory of Computing. Pages 151–158. STOC '71 New York, NY, USA (1971). Association for Computing Machinery.
- [2] Ilya Mironov and Zhang Lintao. "Applications of SAT Solvers to Cryptanalysis of Hash Functions.". In IACR Cryptology ePrint Archive. Volume 2006, pages 102–115. (2006).
- [3] Aarti Gupta, Malay K. Ganai, and Chao Wang. "Sat-based verification methods and applications in hardware verification". In Marco Bernardo and Alessandro Cimatti, editors, Formal Methods for Hardware Verification. Pages 108–143. Berlin, Heidelberg (2006). Springer Berlin Heidelberg.
- [4] Henry Kautz and Bart Selman. "Planning as satisfiability". In Proceedings of the 10th European Conference on Artificial Intelligence. Page 359–363. ECAI '92 USA (1992). John Wiley & Sons, Inc.
- [5] Pey-Chang Lin and Sunil Khatri. "Efficient cancer therapy using Boolean networks and Max-SAT-based ATPG". 2011 IEEE International Workshop on Genomic Signal Processing and Statistics (GENSIPS) Pages 87–90 (2011).
- [6] Martin D Davis, George Logemann, and Donald W Loveland. "A machine program for theorem-proving". Commun. ACM **5**, 394–397 (1962).
- [7] S Kirkpatrick, C D Gelatt, and M P Vecchi. "Optimization by Simulated Annealing". Science **220**, 671–680 (1983).
- [8] Walter Vinci and Daniel Lidar. "Non-stoquastic interactions in quantum annealing via the aharonov-anandan phase". npj Quantum Information (2017).
- [9] Dorit Aharonov, Wim van Dam, Julia Kempe, Zeph Landau, Seth Lloyd, and Oded Regev. "Adiabatic Quantum Computation Is Equivalent to Standard Quantum Computation". SIAM Review **37** (2004).
- [10] James King, Sheir Yarkoni, Jack Raymond, Isil Ozfidan, Andrew King, Mayssam Nevisi, Jeremy Hilton, and Catherine McGeoch. "Quantum Annealing amid Local Ruggedness and Global Frustration". Journal of the Physical Society of Japan **88** (2017).
- [11] Lov K Grover. "A Fast Quantum Mechanical Algorithm for Database Search". In Proceedings of the Twenty-Eighth Annual ACM Symposium on Theory of Computing.

- Pages 212–219. STOC '96 New York, NY, USA (1996). Association for Computing Machinery.
- [12] Thomas Gabor, Sebastian Zielinski, Sebastian Feld, Christoph Roch, Christian Seidel, Florian Neukart, Isabella Galter, Wolfgang Mauere, and Claudia Linnhoff-Popien. “Assessing Solution Quality of 3SAT on a Quantum Annealing Platform” (2019).
- [13] Nouredine Bouhmala. “Combining simulated annealing with local search heuristic for MAX-SAT”. *Journal of Heuristics* **25**, 1–23 (2019).
- [14] Siddhartha Santra, Gregory Quiroz, Greg Ver Steeg, and Daniel Lidar. “Max 2-SAT with up to 108 qubits”. *New Journal of Physics* **16** (2014).
- [15] Alberto Laporati and Sara Felloni. “Three quantum algorithms to solve 3-SAT”. *Theoretical Computer Science* **372**, 218–241 (2007).
- [16] Nicolas J Cerf, Lov K Grover, and Colin P Williams. “Nested quantum search and structured problems”. *Physical Review* **A61** (2000).
- [17] Sheng-Tzong Cheng and Ming-Hung Tao. “Quantum cooperative search algorithm for 3-SAT”. *Journal of Computer and System Sciences* **73**, 123–136 (2007).
- [18] Runkai Zhang, Jing Chen, and Huiling Zhao. “Procedure of Solving 3-SAT Problem by Combining Quantum Search Algorithm and DPLL Algorithm”. In *Performance and Communication Systems*. (2020).
- [19] Bin Yan and Nikolai A. Sinitsyn. “An adiabatic oracle for Grover’s algorithm” (2022). [arXiv:2207.05665](https://arxiv.org/abs/2207.05665).
- [20] Jose J Paulet, Luis F LLana, Hernán Indíbil Calvo, Mauro Mezzini, Fernando Cuartero, and Fernando L Pelayo. “Heuristics for Quantum Computing Dealing with 3-SAT”. *Mathematics* **11** (2023).
- [21] Amit Verma, Mark W Lewis, and Gary A Kochenberger. “Efficient QUBO transformation for Higher Degree Pseudo Boolean Functions” (2021).
- [22] Christian Kofler, Peter Greistorfer, Haibo Wang, and Gary Kochenberger. “A penalty function approach to max 3-sat problems”. Working Paper Series, Social and Economic Sciences 2014-04. Faculty of Social and Economic Sciences, Karl-Franzens-University Graz (2014).
- [23] I Rosenberg. “Reduction of bivalent maximization to the quadratic case”. *Cahiers du Centre d’Études de Recherche Opérationnelle* **17** (1975).
- [24] Amit Verma and Mark W Lewis. “Optimal quadratic reformulations of fourth degree Pseudo-Boolean functions”. *Optimization Letters* **14**, 1557–1569 (2020).
- [25] Lov K Grover. “Quantum Computers Can Search Rapidly by Using Almost Any Transformation”. *Physical Review Letters* **80**, 4329–4332 (1998).
- [26] David Biron, Ofer Biham, Eli Biham, Markus Grassl, and Daniel Lidar. “Generalized Grover Search Algorithm for Arbitrary Initial Amplitude Distribution”. *Lecture Notes in Computer Science* **1509** (1998).
- [27] Xiaoyu Li, Guowu Yang, Carlos Torres, Desheng Zheng, and Kang Wang. “a Class of Efficient Quantum Incrementer Gates for Quantum Circuit Synthesis”. *International Journal of Modern Physics* **B28** (2013).
- [28] David Mitchell, Bart Selman, and Hector Levesque. “Hard and Easy Distributions of SAT Problems”. In *Proceedings Tenth National Conference on Artificial Intelligence*. (1992).
- [29] Massimo Lauria, Jan Elffers, Jakob Nordström, and Marc Vinyals. “Cnfgn: A generator of crafted benchmarks”. In Serge Gaspers and Toby Walsh, editors, *Theory and Applications of Satisfiability Testing – SAT 2017*. Pages 464–473. Cham (2017). Springer International Publishing.
- [30] J J Paulet. “Hybrid Quantum Algorithm for Solving 3-SAT: Quantum Annealing and Circuit Model Quantum Search”. <https://github.com/Paulet02/quantum-annealing-circuit-3sat> (2023).
- [31] Sudip Mukherjee and Bikas Chakrabarti. “Multivariable Optimization: Quantum Annealing & Computation”. *The European Physical Journal Special Topics* **224** (2014).

[32] Dennis Willsch, Madita Willsch, Carlos Gonzalez Calaza, Hans Raedt, Marika Svensson, and Kristel Michiels. “Benchmarking Advantage and D-Wave 2000Q

quantum annealers with exact cover problems” (2021).

A DWave’s quantum annealing belongs to $O(n)$

As shown in [31], simulated annealing and quantum annealing are conceptually equivalent.

Each task performed on DWave quantum annealers takes a total time of qpu_access_time . This time is divided into $qpu_programming_time$ and $qpu_sampling_time$ as we can see in fig. 17. The $qpu_programming_time$ is the time performed once at initializing stage of the QPU (regardless the number of measured qubits or the number of executions or any other issue), and the $qpu_sampling_time$ is the time for multiple sampling times within the current execution on the QPU. Fig. 19 shows a more detailed information of it.

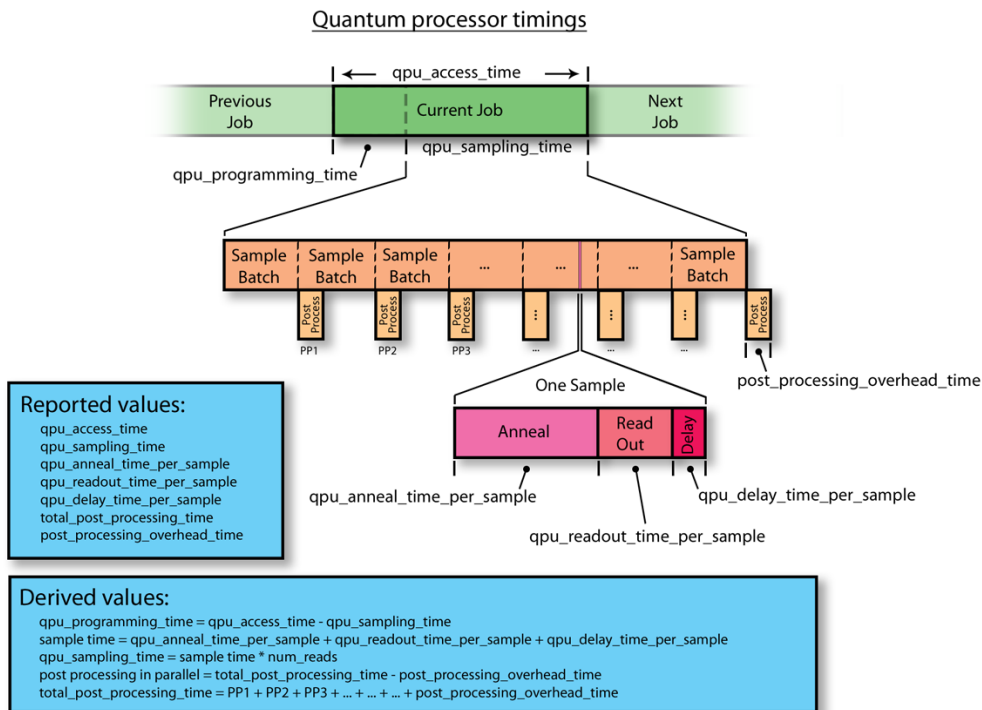


Figure 17: D-Wave QPU timing structure. Image from <https://docs.dwavesys.com/>

For that, the resulting qpu_access_time is:

$$T = T_p + \Delta + T_s \quad (34)$$

Where T_p is $qpu_programming_time$ and T_s is $qpu_sampling_time$. Δ stands for an initialization time spent in low-level operations.

We estimated that the most accurate hardware option within D-Wave offer is DW_2000Q_6 . In fact, as shown in [32] *D-Wave 2000Q* systems overcome *D-Wave Advantage* at accuracy when dealing with sparsely connected problems as for example that which is depicted in fig. 18 which corresponds to one of our examples with 7 variables. Let’s notice that although the maximum number of variables in our work reaches 22 the density prevent them from being non-sparse.

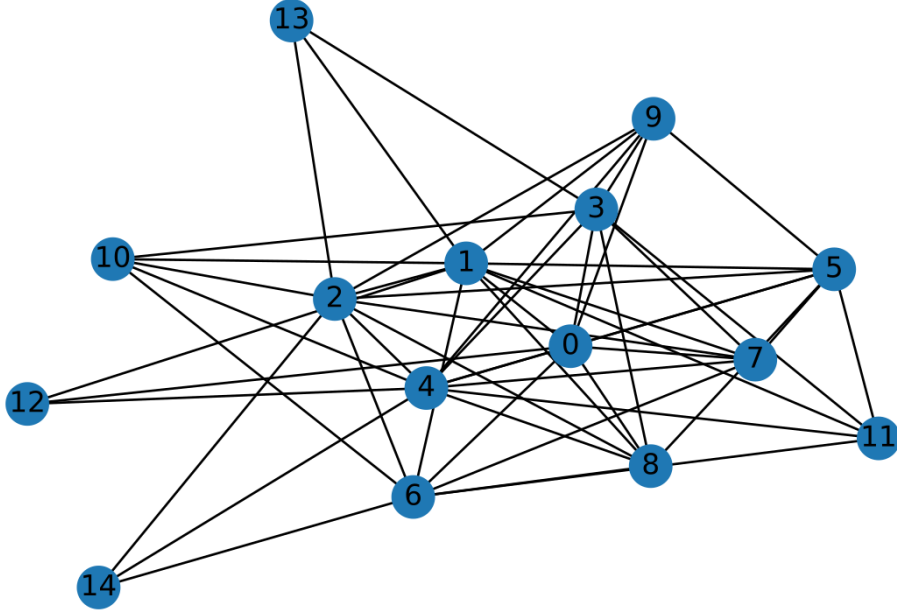


Figure 18: 7 variables 3-SAT problem converted to MaxSAT and codified as a graph

The $qpu_sampling_time$, T_s , is the time which determines the complexity. This time can be decomposed into:

$$T_s = (T_a + T_r + T_d) \cdot R \quad (35)$$

Where T_a is the single-sample annealing time, T_r is the single-sample readout time and T_d is the single-sample delay time, which consists of the following optional components:

$$T_d = readout_thermalization + reduce_intersample_correlation + reinitialize_state \quad (36)$$

In a nutshell:

- T : Total time of execution on the QPU.
- T_p : Total time to program the QPU. It depends on the *programming_thermalization*, that is the time to wait after programming the QPU to cool back to base temperature. The value of the *programming_thermalization* parameter is the default one.
- T_s : Total time for all samples.
- R : Number of samples. In our case the number of samples equals the **number of variables in the QUBO formulation** of the problem.
- T_a : Annealing time per sample. In our case is the one by **default**.
- T_d : Delay between each pair of consecutive samples:
 - *readout_thermalization*: Time to wait after each measurement of a qubit for it to cool back to base temperature. In our case it is set to $10 \mu s$.
 - *reduce_intersample_correlation*: Delay time added after each anneal for the sake of removing the effects from previous measurements of qubits. Adds a delay times before each anneal to lose the effects from the previous read. In our case it is set to **True** and it can be computed as:

$$delay = 500 + \frac{T_{schedule} (10000 - 500)}{2000} \quad (37)$$

Where $T_{schedule}$ is the total time of the anneal schedule.

– *reinitialize_state*: Time only used for reverse annealing. In our case it is set to **False**

- T_r : Time per sample read. Depends on the number of qubits.

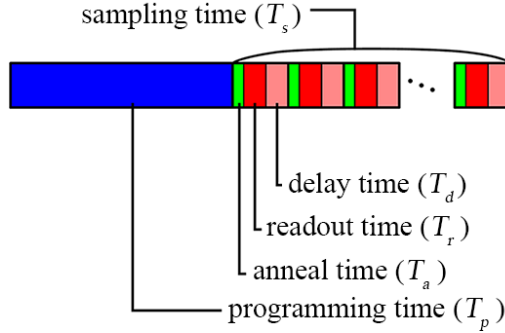


Figure 19: Detail of QPU access time. Image from <https://docs.dwavesys.com/>

Fig. 20 shows the average time taken for the execution of the testbed described in section 4.

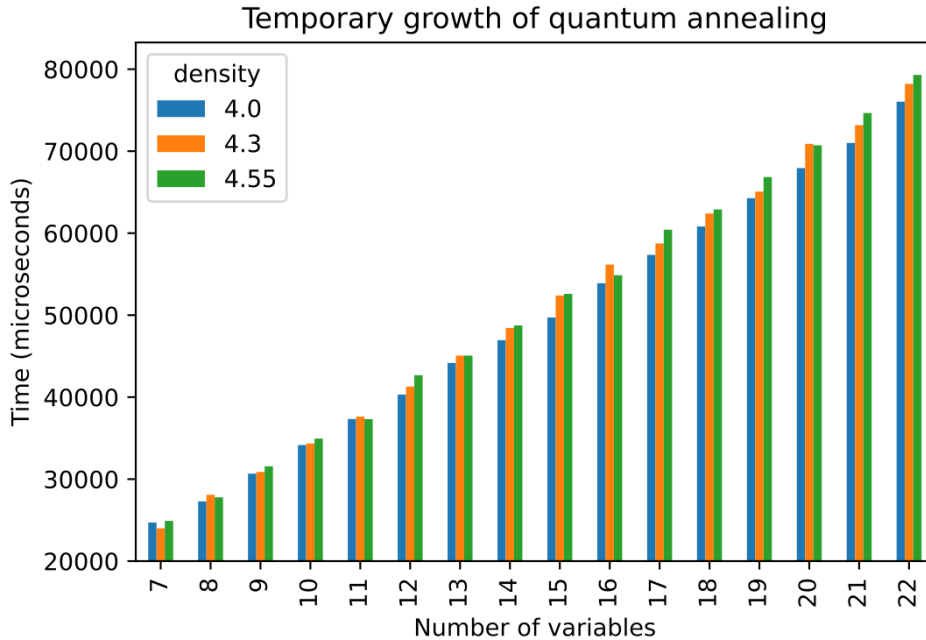


Figure 20: Average QPU access time for testing

B Simulated annealing belongs to $O(n)$

Each of the 5 executions of each of the 480 examples depends on three parameters, in a similar way to quantum annealing. These three parameters are:

- *num_reads*: Number of executions of the simulated annealing algorithm. In our case it is set to the **number of variables in the QUBO formulation** of the problem (same as for quantum annealing).
- *num_sweeps*: Number of steps in which the annealing protocol is divided. In our case it is set to **default** (same as for quantum annealing).
- *num_sweeps_per_beta*: Number of steps performed in each step of the annealing protocol. In our case it is set to **1**.

Thus, the complexity will depend on $O(num_reads \cdot num_sweeps \cdot num_sweeps_per_beta)$. Fig. 21 shows the average time taken by the execution of the setups described in section 4.

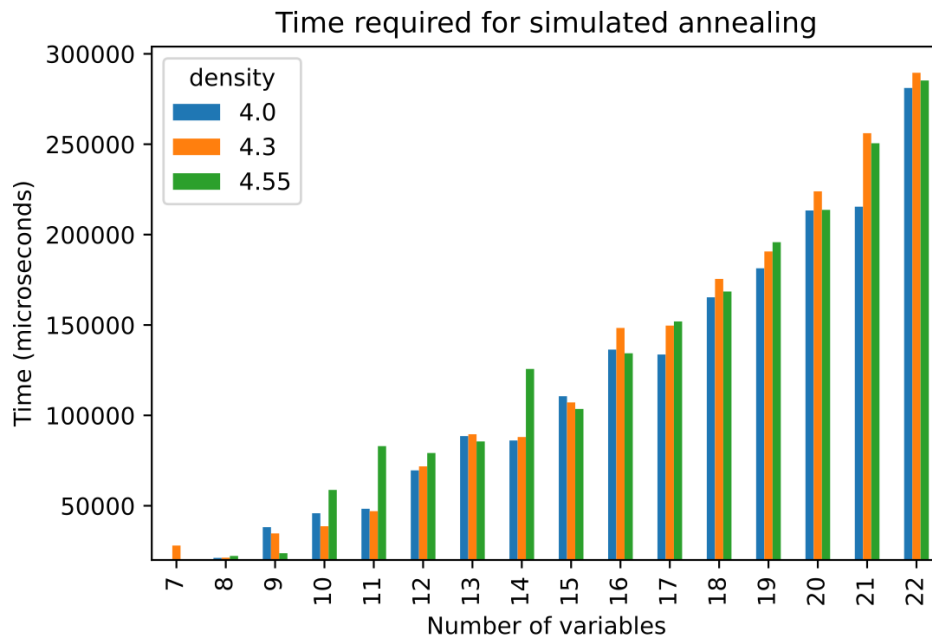


Figure 21: Average execution time within our testbed

C Accuracy of both annealing processes

The following table compares Hamming and Cyclical distances between the state provided by each of the annealing options and, the solution state of the problem:

Number of variables	Hamming distance		Cyclical distance	
	Quantum annealing	Simulated annealing	Quantum annealing	Simulated annealing
7	1.33	0.27	13.73	2.49
8	1.03	0.19	19.23	7.23
9	1.9	0.37	73.5	10.59
10	3.03	0.47	174.23	24.35
11	3.83	0.64	357.6	90.72
12	3.7	1.02	820.43	189.55
13	4.17	1.22	1637.63	494.97
14	4.67	1.27	3103.73	936.16
15	4.93	1.95	6256.4	2050.91
16	5.8	2.81	13125.23	6471.44
17	7.03	3.22	30292.83	12988.37
18	7.2	3.81	51982.17	34910.17
19	7.93	3.59	134792.1	49551.77
20	7.33	4.82	254491.07	161184.32
21	8.53	4.77	576134.93	260356.66
22	8.73	5.25	1013263.87	563339.43

Table 2: Average distances of both annealing processes

D Quantum circuit-model search results

The following table compares Hamming and Cyclical quantum search proposed strategies with respect to original Grover’s algorithm. Each of the strategies has been split into the case of knowing in advance the corresponding distance between annealing output state and actual solution state, and, not knowing that value in advance:

Number of variables	Density	Grover’s algorithm		Hamming quantum search		Cyclical quantum search	
				Unknown distance	Known distance	Unknown distance	Known distance
7	4.0	8.0	0.0%	2.42 -69.75%	0.85 -89.42%	1.32 -83.5%	0.78 -90.25%
7	4.3	8.0	0.0%	0.68 -91.5%	0.32 -95.97%	0.24 -97.0%	0.24 -97.0%
7	4.55	8.0	0.0%	0.88 -89.0%	0.51 -93.59%	0.48 -94.0%	0.44 -94.5%
8	4.0	12.0	0.0%	1.02 -91.5%	0.57 -95.22%	1.12 -90.67%	0.6 -95.0%
8	4.3	12.0	0.0%	0.44 -96.33%	0.38 -96.83%	1.12 -90.67%	1.0 -91.67%
8	4.55	12.0	0.0%	0.92 -92.33%	0.68 -94.32%	1.92 -84.0%	1.52 -87.33%
9	4.0	17.0	0.0%	2.4 -85.88%	1.09 -93.58%	1.68 -90.12%	1.06 -93.76%
9	4.3	17.0	0.0%	4.68 -72.47%	2.12 -87.51%	2.64 -84.47%	1.64 -90.35%
9	4.55	17.0	0.0%	1.1 -93.53%	0.78 -95.41%	1.68 -90.12%	0.78 -95.41%
10	4.0	25.0	0.0%	4.92 -80.32%	1.9 -92.39%	3.74 -85.04%	2.74 -89.04%
10	4.3	25.0	0.0%	8.56 -65.76%	3.93 -84.29%	4.08 -83.68%	2.84 -88.64%
10	4.55	25.0	0.0%	1.5 -94.0%	0.18 -99.27%	0.34 -98.64%	0.34 -98.64%
11	4.0	35.0	0.0%	8.08 -76.91%	3.29 -90.6%	8.0 -77.14%	5.06 -85.54%
11	4.3	35.0	0.0%	7.26 -79.26%	3.27 -90.65%	8.5 -75.71%	6.1 -82.57%
11	4.55	35.0	0.0%	9.26 -73.54%	3.42 -90.22%	5.5 -84.29%	3.32 -90.51%
12	4.0	50.0	0.0%	15.78 -68.44%	5.4 -89.2%	9.8 -80.4%	6.64 -86.72%
12	4.3	50.0	0.0%	30.7 -38.6%	9.19 -81.63%	14.7 -70.6%	9.8 -80.4%
12	4.55	50.0	0.0%	12.38 -75.24%	4.89 -90.23%	9.1 -81.8%	5.5 -89.0%
13	4.0	71.0	0.0%	46.38 -34.68%	16.19 -77.2%	32.0 -54.93%	20.46 -71.18%
13	4.3	71.0	0.0%	23.64 -66.7%	6.23 -91.23%	17.0 -76.06%	9.98 -85.94%
13	4.55	71.0	0.0%	10.92 -84.62%	5.69 -91.98%	18.0 -74.65%	7.34 -89.66%
14	4.0	100.0	0.0%	45.6 -54.4%	15.44 -84.56%	25.56 -74.44%	17.06 -82.94%
14	4.3	100.0	0.0%	35.46 -64.54%	12.87 -87.13%	32.66 -67.34%	22.34 -77.66%
14	4.55	100.0	0.0%	37.04 -62.96%	18.7 -81.3%	22.72 -77.28%	13.86 -86.14%

Table 3: Total iterations results for 7 to 14 variables

Number of variables	Density	Grover's algorithm		Hamming quantum search		Cyclical quantum search	
				Unknown distance	Known distance	Unknown distance	Known distance
15	4.0	142.0	0.0%	126.94 -10.61%	38.74 -72.72%	70.0 -50.7%	45.42 -68.01%
15	4.3	142.0	0.0%	79.02 -44.35%	25.84 -81.8%	44.0 -69.01%	27.34 -80.75%
15	4.55	142.0	0.0%	60.2 -57.61%	22.2 -84.36%	28.0 -80.28%	18.42 -87.03%
16	4.0	201.0	0.0%	144.36 -28.18%	44.04 -78.09%	79.52 -60.44%	57.68 -71.3%
16	4.3	201.0	0.0%	143.98 -28.37%	41.69 -79.26%	88.04 -56.2%	57.46 -71.41%
16	4.55	201.0	0.0%	240.12 +19.46%	64.23 -68.05%	99.4 -50.55%	74.68 -62.85%
17	4.0	284.0	0.0%	417.28 +46.93%	136.04 -52.1%	225.12 -20.73%	154.1 -45.74%
17	4.3	284.0	0.0%	179.84 -36.68%	65.99 -76.76%	124.62 -56.12%	59.74 -78.96%
17	4.55	284.0	0.0%	128.36 -54.8%	49.54 -82.56%	124.62 -56.12%	71.5 -74.82%
18	4.0	402.0	0.0%	415.18 +3.28%	140.15 -65.14%	238.56 -40.66%	165.06 -58.94%
18	4.3	402.0	0.0%	377.02 -6.21%	107.89 -73.16%	210.16 -47.72%	131.36 -67.32%
18	4.55	402.0	0.0%	453.74 +12.87%	158.91 -60.47%	266.96 -33.59%	188.64 -53.07%
19	4.0	568.0	0.0%	541.06 -4.74%	159.3 -71.95%	393.96 -30.64%	225.36 -60.32%
19	4.3	568.0	0.0%	348.6 -38.63%	118.28 -79.18%	281.4 -50.46%	177.86 -68.69%
19	4.55	568.0	0.0%	470.74 -17.12%	170.67 -69.95%	257.28 -54.7%	156.56 -72.44%
20	4.0	804.0	0.0%	1156.86 +43.89%	337.54 -58.02%	624.8 -22.29%	405.58 -49.55%
20	4.3	804.0	0.0%	749.66 -6.76%	258.34 -67.87%	590.72 -26.53%	410.28 -48.97%
20	4.55	804.0	0.0%	923.16 +14.82%	303.85 -62.21%	477.12 -40.66%	330.5 -58.89%
21	4.0	1137.0	0.0%	1429.72 +25.74%	412.86 -63.69%	755.76 -33.53%	528.68 -53.5%
21	4.3	1137.0	0.0%	662.64 -41.72%	276.12 -75.72%	755.76 -33.53%	456.82 -59.82%
21	4.55	1137.0	0.0%	1297.7 +14.13%	379.97 -66.58%	836.16 -26.46%	547.52 -51.85%
22	4.0	1608.0	0.0%	2036.14 +26.63%	633.04 -60.63%	932.34 -42.02%	604.42 -62.41%
22	4.3	1608.0	0.0%	1947.88 +21.14%	638.87 -60.27%	1273.44 -20.81%	714.5 -55.57%
22	4.55	1608.0	0.0%	1516.18 -5.71%	559.94 -65.18%	1182.48 -26.46%	720.12 -55.22%

Table 4: Total iterations results for 15 to 22 variables